(20). Pemetrexed treatment may influence adduct formation by cisplatin or the repair of formed adducts, because pemetrexed inhibits both pyrimidine and purine synthesis. The disturbances of the cell cycle produced by pemetrexed and cisplatin may also influence the cytotoxic effects of each other because these agents are cell cycle specific (21,22).

These suggest that the drug schedule may play a significant role in the outcome, and therefore the design of a protocol using them in combination may requires careful consideration. Schedule-dependent interactions have been observed for the combinations of pemetrexed and gemcitabine (23), doxorubicin (24), or paclitaxel (25) in in vitro studies. Because experimental studies for the combination of pemetrexed with cisplatin are limited (26, 27), the optimal schedule of this combination is obscure.

The present study aimed at elucidating the cytotoxic effects of combinations of pemetrexed and cisplatin in various schedules on four human carcinoma cell lines. Our data suggest that the simultaneous administration of pemetrexed and cisplatin may be suboptimal for this combination and the optimal schedule of this combination at the cellular level is the sequential administration of pemetrexed followed by cisplatin.

MATERIALS AND METHODS

Cell Lines

The human lung cancer A549, the breast cancer MCF7, the ovarian cancer PA1, and the colon cancer WiDr cells were used. These cells were obtained from the American Type Culture Collection (Rockville, MD) and maintained in RPMI-1640 medium (Sigma Chemical Co., St Louis, MO) supplemented with 10% heat-inactivated fetal bovine serum (FBS) (Grand Island Biological Co.) and antibiotics. The doubling times of A549, MCF7, PA1, and WiDr cells in our experimental conditions were 20–24 h.

Drugs

Pemetrexed was kindly provided by Eli Lilly and Company (Indianapolis, IN). Cisplatin was purchased from Nihon Kayaku Co. (Tokyo). Drugs were diluted with RPMI-1640 plus 10% FBS.

Cell Growth Inhibition Using Combined Anticancer Agents

On day 0, cells growing in the exponential phase were harvested with 0.05% trypsin and 0.02% EDTA and resuspended to a final concentration of 5.0×10^3 cells/ml in fresh medium containing 10% FBS and antibiotics. The cell suspensions (100 μl) were dispensed using a multichannel pipette into the individual wells of a 96-well tissue culture plate with a lid (Falcon, Oxnard, CA). Each plate had one 8-well control column containing medium alone and one 8-well control column containing cells without drug. Eight plates were prepared for each drug combination. The cells were preincubated overnight to allow attachment.

Simultaneous Exposure to Pemetrexed and Cisplatin

After 16–20-h incubation for cell attachment, solutions of pemetrexed and cisplatin (50 μl) at different concentrations were added to the individual wells. The plates were also incubated under the same conditions for 24 h. The cells were then washed twice with culture medium containing 1% FBS, and then fresh medium containing 10% FBS (200 μl) and antibiotics was added. The cells were incubated again for 4 days.

Sequential Exposure to Pemetrexed Followed by Cisplatin or Vice Versa

After 16–20-h incubation, medium containing 10% FBS (50 μl) and solutions (50 μl) of pemetrexed (or cisplatin) at different concentrations was added to the individual wells. The plates were then incubated under the same conditions for 24 h. The cells were washed

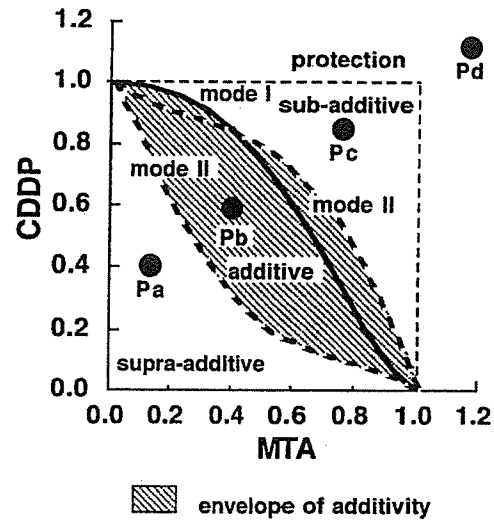

Figure 1. Schematic representation of an isobologram (29). The envelope of additivity, surrounded by mode I (solid line) and mode II (dotted lines) isobologram lines, was constructed from the dose–response curves of pemetrexed (MTA) and cisplatin (CDDP). The concentrations that produced 80% cell growth inhibition were expressed as 1.0 in the ordinate and the abscissa of all isobolograms for MCF7, PA1, and WiDr cells, while the concentrations that produced 50% cell growth inhibition were expressed as 1.0 in the ordinate and the abscissa of all isobolograms for A549 cells. The combined data points Pa, Pb, Pc, and Pd show supra-additive, additive, subadditive, and protective effects, respectively.

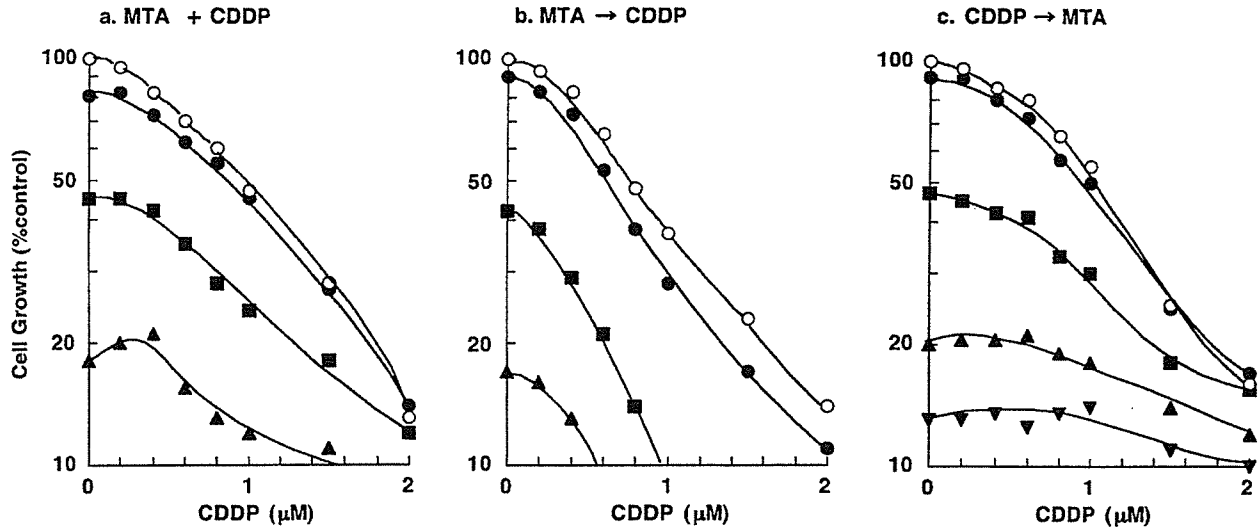

Figure 2. Schedule dependence of the interaction between pemetrexed and cisplatin in PA1 cells. Cells were exposed to these two drugs simultaneously for 24 h (a), pemetrexed first for 24 h followed by cisplatin for 24 h (b), or the reverse sequence (c). The cell number after 5 days was measured using the MTT assay and was plotted as a percentage of the control (cells not exposed to drugs). The concentrations of cisplatin are shown on the abscissa. The concentrations of pemetrexed were 0 (open circles), 20 (filled circles), 50 (filled squares), 100 (filled upward triangles), and 200 (filled downward triangles) nM, respectively. Data are mean values for three independent experiments; SE was <20%.

twice with culture medium containing 1% FBS; fresh medium containing 10% FBS (150 μl) and antibiotics was added, followed by the addition of solutions (50 μl) of cisplatin (or pemetrexed) at different concentrations. The plates were incubated again under the same conditions for 24 h. The cells were then washed twice with culture medium, and fresh medium containing 10% FBS (200 μl) and antibiotics was added. The cells were then incubated again for 3 days.

MTT Assay

The cytotoxicity of pemetrexed alone, cisplatin alone, and their combinations was determined by 3-(4,5-dimethylthiazol-2-yl)-2,5-diphenyltetrazolium bromide (MTT) assay as described previously (28). For all four cell lines examined, we were able to establish a linear relationship between the MTT assay value and the cell number within the range shown.

Isobologram

The dose–response interactions between pemetrexed and cisplatin for the MCF7, PA1, and WiDr cells were evaluated at the IC_{80} level by the isobologram method of Steel and Peckham (Fig. 1) (29). The IC_{80} was defined as the concentration of drug that produced 80% cell growth inhibition (i.e., an 80% reduction in absorbance). Although the drug interaction at IC_{90} or more would be more important than both IC_{80} and IC_{50} for cancer chemotherapy, it is difficult to get reliable data at IC_{90} or more using MTT assay. A549 was resistant to pemetrexed and the interactions between them were evaluated at the IC_{50} level.

We used the isobologram method of Steel and Peckham because this method can cope with any agents with unclear cytotoxic mechanisms and a variety of dose–response curves of anticancer agents. The concept and analysis of the isobologram has been described in detail previously (30,31). The isobologram of Steel and Peckham is very strict for synergism and antagonism.

If the two agents act additively by independent mechanisms, the combined data points would lie near the mode I line (hetero-addition). If the agents act additively by similar mechanisms, the combined data points would lie near the mode II lines (iso-addition). When the data points of the drug combination fell within the area surrounded by mode I and /or mode II lines (i.e., within the envelope of additivity), the combination was described as additive.

A combination that gives data points to the left of the envelope of additivity (i.e., the combined effect is caused by lower doses of the two agents than is predicted) can confidently be described as supra-additive (synergism). A combination that gives data points to the right of the envelope of additivity, but within the square or on the line of the square, can be described as subadditive (i.e., the combination is superior or equal to a single agent but is less than additive). A combination that gives

data points outside the square can be described as protective (i.e., the combination is inferior in cytotoxic action to a single agent). A combination with both subadditive and/or protective interactions can confidently be described as antagonistic.

Data Analysis

The findings were analyzed as described previously (32). When the observed data points from combinations fell mainly in the area of supra-additivity or in the areas of subadditivity and protection, the mean value of the observed data was smaller than that of the predicted minimum data or larger than that of the predicted maximum data, the combinations were considered to have a synergistic or an antagonistic effect, respectively. To determine whether the condition of synergism (or antagonism) truly existed, a Wilcoxon signed-rank test was performed to compare the observed data with the predicted minimum (or maximum) data for an additive effect. Probability values of $p < 0.05$ were considered significant. Because the isobologram of Steel and Peckham is very strict for synergism and antagonism, combinations with $p \geq 0.05$ were defined as having an additive/synergistic (or additive/antagonistic) effect. All statistical analyses were performed using the Stat View 4.01 software program (Abacus Concepts, Berkeley, CA).

Flow Cytometric Analysis

PA1 cells were treated with 0.2 μM pemetrexed alone or 0.5 μM cisplatin alone or their combination simultaneously for 24 h. MCF7 cells were treated with 0.5 μM pemetrexed alone or 5 μM cisplatin alone or their combination simultaneously for 24 h. The cells were also treated with pemetrexed for 24 h followed by cisplatin for 24 h or the reverse sequence. The cells were harvested at 48 h and the cell cycle profiles were analyzed by staining the intracellular DNA with propidium iodide in preparation for flow cytometry with the FACScan CellFIT system (Becton-Dickinson, San Jose, CA). A DNA histogram was obtained by analyzing 25,000 cells with the ModFIT program (Becton-Dickinson) (33).

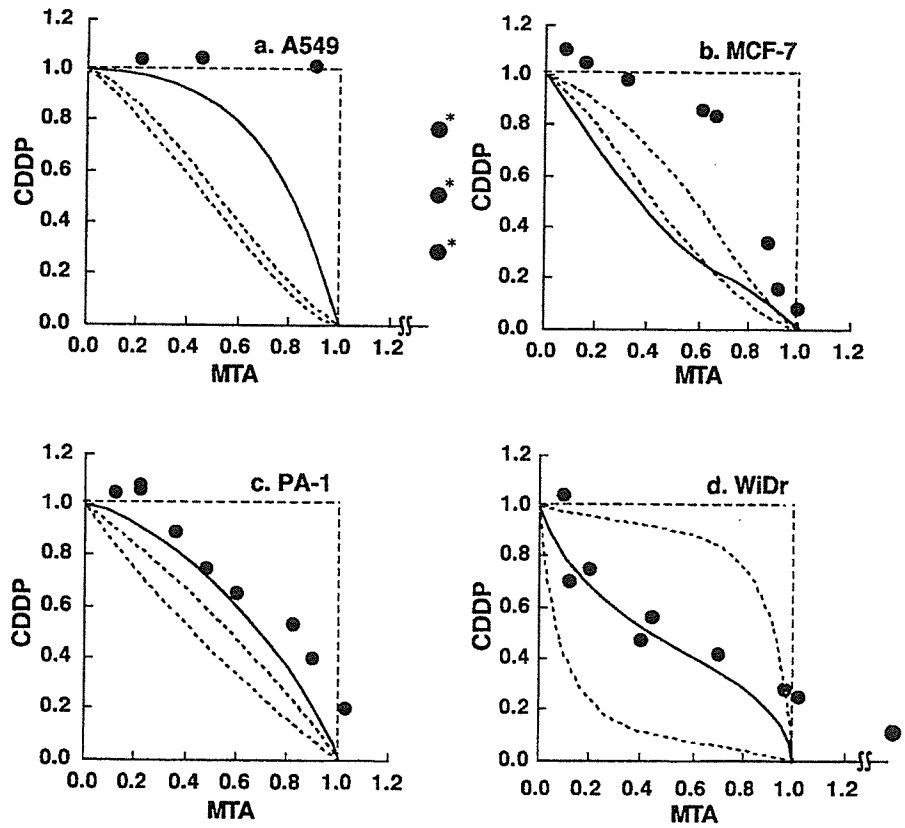

Figure 3. Isobolograms of simultaneous exposure to pemetrexed and cisplatin for 24 h in A549 (a), MCF7 (b), PA1 (c), and WiDr (d) cells. For the A549, MCF7, and PA1 cells, the combined data points fell in the areas of subadditivity and protection. For the WiDr cells, the combined data points fell mainly within the envelope of additivity. Data are mean values for at least three independent experiments; SE was <25% (*except the data).

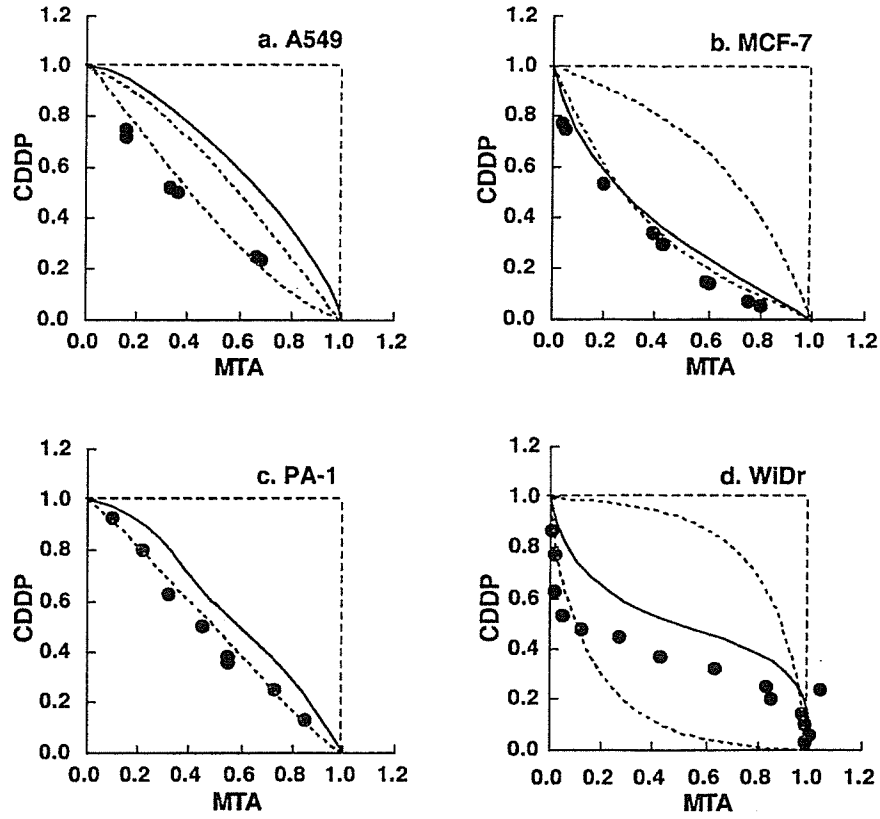

Figure 4. Isobolograms of sequential exposure to pemetrexed (24 h) followed by cisplatin (24 h) in A549 (a), MCF7 (b), PA1 (c), and WiDr (d) cells. For the A549, MCF7, and PA1 cells, all or most of the data points of the combinations fell within the envelope of additivity and in the area of supra-additivity. For the WiDr cells, most of the data points fell within the envelope of additivity. Data are mean values for at least three independent experiments; SE was <20%.

RESULTS

The IC_{80} values of 24-h exposure to pemetrexed for A549, MCF7, PA1, and WiDr cells were >5, 2.5 ± 0.4, 0.10 ± 0.03, and 0.55 ± 0.2 μM, respectively. Because A549 cells were resistant to pemetrexed and the IC_{80} level was not obtained, the interactions between pemetrexed and cisplatin were evaluated at the IC_{50} level. The IC_{50} value of 24-h exposure to pemetrexed for A549 cells was 2.7 ± 0.3 μM.

Figure 2 shows the dose–response curves obtained from simultaneous exposure and sequential exposure to pemetrexed and cisplatin for the PA1 cells. The dose–response curves were plotted on a semilog scale as a percentage of the control, the cell number of which was obtained from the samples not exposed to the drugs administered simultaneously. Dose–response curves in which the pemetrexed concentrations are shown on the abscissa could be made based on the same data (figure not shown). Based upon the dose–response curves of pemetrexed alone and cisplatin alone, three isoeffect curves (mode I and mode II lines) were constructed. Isobolograms at the IC_{80} or IC_{50} levels were generated based upon these dose–response curves for the combinations.

Simultaneous Exposure to Pemetrexed and Cisplatin

Figure 3 shows isobolograms of the A549, MCF7, PA1, and WiDr cells after simultaneous exposure to pemetrexed and cisplatin for 24 h. For the A549, MCF7, and PA1 cells, the combined data points fell in the areas of subadditivity and protection, respectively. The mean values of the observed data (>1.15, 0.95, and 0.69) were larger than those of the predicted maximum values (0.75, 0.72, and 0.56). The observed data and the predicted maximum data were compared by the Wilcoxon signed-rank test. The differences were significant ($p < 0.05$, $p < 0.02$, and $p < 0.01$), indicating antagonistic effects (Table 1). For the WiDr cells, the combined data points fell mainly within the envelope of additivity. The mean values of the observed data (0.66) were larger than those of the predicted minimum values (0.27), and smaller than those of the predicted maximum values (0.73), indicating additive effects.

Sequential Exposure to Pemetrexed Followed by Cisplatin

Figure 4 shows isobolograms of the A549, MCF7, PA1, and WiDr cells exposed first to pemetrexed for 24 h and then cisplatin for 24 h. For the MCF7 cells, combined data points fell in the area of supra-additivity. The mean values of the observed data (0.40) were smaller than those of the predicted minimum values (0.44) (Table 1). The difference between them was significant ($p < 0.01$), indicating synergistic effects. For the A549 and PA1 cells, combined data points fell in the area of supra-additivity and within the envelope of additivity. The mean values of the observed data were smaller than those of the predicted minimum values (Table 1), but the differences were not significant ($p > 0.05$ and $p > 0.05$), indicating additive/synergistic effects. For the WiDr cells, the combined data points fell within the envelope of additivity and in the areas of supra-additivity and protection. The mean value of the observed data was smaller than the predicted maximum values and larger than that of the predicted minimum values (Table 1), indicating additive effects.

Sequential Exposure to Cisplatin Followed by Pemetrexed

Figure 5 shows isobolograms of the four cell lines exposed first to cisplatin for 24 h and then pemetrexed for 24 h. For the A549, MCF7, and PA1 cells, all or most of the combined data points fell in the areas of subadditivity and protection. The mean values of the observed data were larger than those of the predicted maximum values (Table 1). The differences were significant ($p < 0.05$, $p < 0.02$, and $p < 0.02$, respectively), indicating antagonistic effects. For the WiDr cells, most of the combined data points fell within the envelope of additivity, indicating an additive effect of this schedule.

Flow Cytometric Analysis

Finally, we evaluated the cytotoxic effects of pemetrexed and cisplatin on cancer cells using flow cytome-

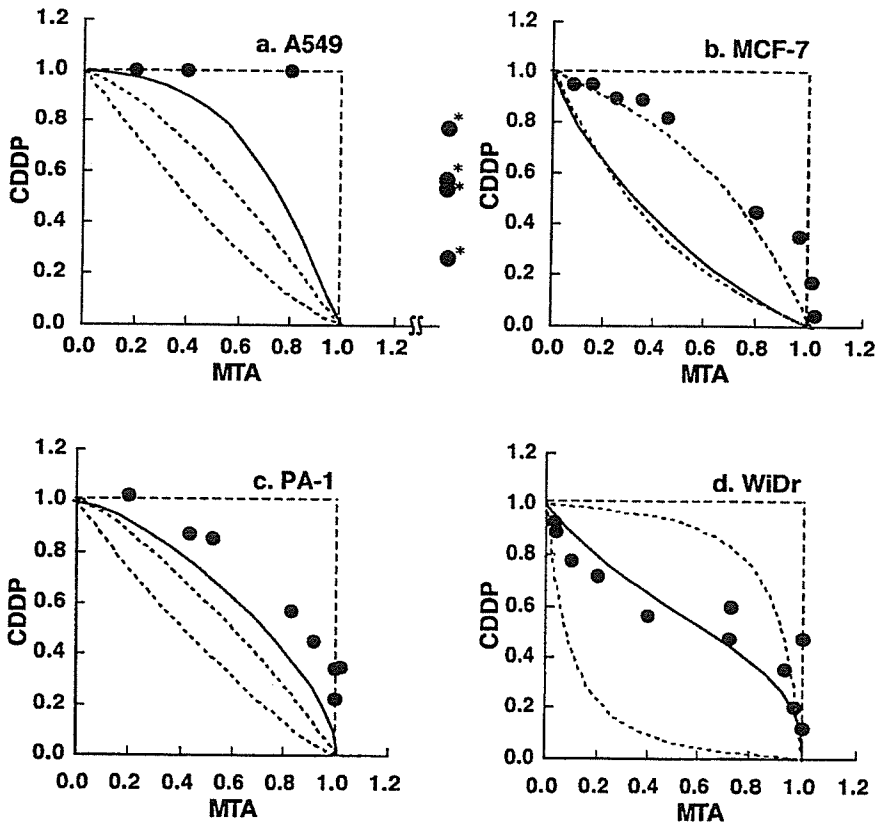

Figure 5. Isobolograms of sequential exposure to cisplatin (24 h) followed by pemetrexed (24 h) in A549 (a), MCF7 (b), PA1 (c), and WiDr (d) cells. For the A549, MCF7, and PA1 cells, all or most of the data points of the combinations fell in the areas of subadditivity and protection. For the WiDr cells, most of the data points of the combinations fell within the envelope of additivity and in the area of subadditivity. Data are mean values for at least three independent experiments; SE was <20%(*except the data).

Table 1. Mean Values of Observed, Predicted Minimum, and Predicted Maximum Data of Pemetrexed (MTA) in Combination With Cisplatin (CDDP) at IC_{80} for MCF7, PA1, and WiDr Cells and at IC_{50} for A549 Cells

Schedule	Cell Line	n	Observed Data	Predictaed Data for an Additive Effect		Effect
				Minimum	Maximum	
MTA + CDDP	A549	6	1.15	0.44	0.75	antagonism ($p < 0.05$)
	MCF7	8	0.95	0.57	0.72	antagonism ($p < 0.02$)
	PA1	9	0.69	0.40	0.56	antagonism ($p < 0.01$)
	WiDr	9	0.66	0.27	0.73	additive
MTA → CDDP	A549+	6	0.45	0.47	0.72	additive/synergism ($p > 0.05$)
	MCF7	9	0.40	0.44	0.78	synergism ($p < 0.01$)
	PA1	8	0.52	0.55	0.64	additive/synergism($p > 0.05$)
	WiDr	15	0.64	0.46	0.84	additive
CDDP → MTA	A549	7	1.14	0.41	0.74	antagonism ($p < 0.05$)
	MCF7	9	0.82	0.52	0.73	antagonism ($p < 0.02$)
	PA1	8	0.75	0.41	0.63	antagonism ($p < 0.02$)
	WiDr	11	0.71	0.21	0.82	additive

try. Cell cycle analysis revealed that pemetrexed and cisplatin arrested PA1 cells in late G_1 to early S phase and G_2/M phase, respectively (Fig. 6A, Table 2). When PA1 cells were exposed to both drugs simultaneously, the cell cycle profile was almost identical to that of a single treatment with pemetrexed, suggesting that the cell cycle effect of pemetrexed is dominant over that of cisplatin. As a result, the apoptosis-inducing effect of cisplatin, which was estimated by an increase in the size of sub-G_1 fraction, was almost completely cancelled in the presence of pemetrexed (Fig. 6A, MTA + CDDP). When PA1 cells were treated with cisplatin first and followed by pemetrexed, the cell cycle pattern closely resembled that of cells treated with cisplatin alone except for a modest increase in G_1 and S phases (Fig. 6A, Table 2, CDDP to MTA). The induction of apoptotsis was less prominent in the CDDP to MTA treatment than in the CDDP treatment (Table 2). In contrast, both apoptosis and G_2/M arrest were enhanced when PA1 cells were treated with pemetrexed first and followed by cisplatin compared with the treatment with either pemetrexed or cisplatin alone (Fig. 6A, Table 2, MTA to CDDP).

We carried out the same analysis with another cancer cell line MCF7 and obtained highly reproducible results. Upon simultaneous addition, the cell cycle effect of cisplatin was almost completely abrogated and the percentage of apoptotic cells was less than that of a single treatment with pemetrexed (Fig. 6B, MTA + CDDP). Similarly, apoptosis was suppressed when MCF7 cells were treated with cisplatin first and followed by pemetrexed compared with the treatment with either pemetrexed or cisplatin alone (Fig. 6B, Table 2, CDDP to MTA). In contrast, the apoptosis-inducing effect of pemetrexed was enhanced by the sequential exposure to cisplatin after pemetrexed (Fig. 6B, Table 2, MTA to CDDP). Overall, these data are fully consistent with the results of isobologram analysis, and provide the molecular basis of the interaction between the two drugs.

DISCUSSION

We found that the cytotoxic interaction between pemetrexed and cisplatin was schedule dependent. Simultaneous exposure to pemetrexed and cisplatin and sequential exposure to cisplatin followed by pemetrexed showed antagonistic effects in A549, MCF7, and PA1 cells, while sequential exposure to pemetrexed followed by cisplatin had a tendency to produce synergistic effects. In the latter schedule, observed data points in A549, MCF7, and PA1 cells were smaller than predicted minimum values for an additive effect (Table 1). WiDr cells showed additive effects in all schedules. The cause of difference in combined effects among cell lines is unknown. The difference may reflect the folate metabolism and the variety of target numbers (enzymes) in the cells. In addition, the isobologram of Steel and Peckham is stricter for synergism and antagonism than other methods. This may also influence the results.

In general, it is difficult to clarify the mechanisms underlying the drug combination. In this study, however, cell cycle analysis provided a clue to understand the molecular basis of schedule-dependent synergism and antagonism of the combination of pemetrexed and cisplatin. The exposure of PA1 and MCF7 cells to pemetrexed for 24 h led to a synchronization of most cells in late G_1 to

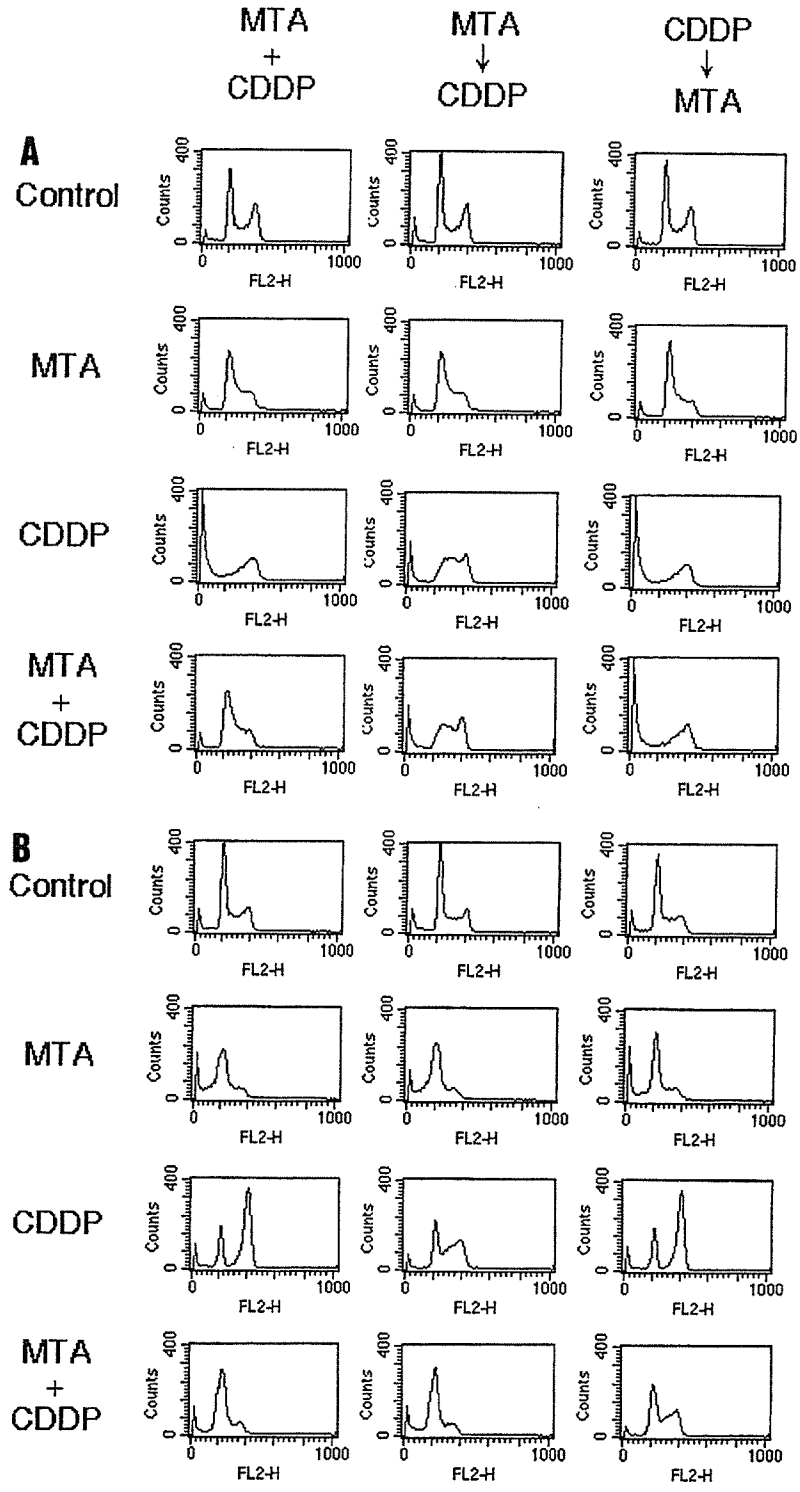

Figure 6. Flow cytometric analysis of cell cycle perturbation. PA1 cells, treated with 0.2 μM pemetrexed (MTA), 0.5 μM cisplatin (CDDP), both drugs simultaneously for 24 h, pemetrexed for 24 h followed by cisplatin for 24 h, or the reverse sequence were harvested at 48 h (A), and MCF7 cells, treated with 0.5 μM pemetrexed (MTA), 5 μM cisplatin (CDDP), both drugs simultaneously for 24 h, pemetrexed for 24 h followed by cisplatin for 24 h, or the reverse sequence were harvested at 48 h (B) and stained for DNA with propidium iodide and analyzed by flow cytometry as described in Materials and Methods.

Table 2. Cell Cycle Perturbations Induced by Pemetrexed (MTA), Cisplatin (CDDP), and Their Combinations for PA1 and MCF7 Cells at 48 h

	MTA + CDDP (24 h)				MTA (24 h) → CDDP (24 h)				CDDP (24 h)→ MTA (24 h)			
Cell Cycle (%)	Control	MTA	CDDP	MTA + CDDP	Control	MTA	CDDP	MTA + CDDP	Control	MTA	CDDP	MTA + CDDP
PA1 cells												
Sub-G_1	3.6	2.4	42.9	2.1	4.3	3.1	8.9	15.3	2.9	2.2	45.1	41.8
G_1	56.2	64.1	7.3	67.1	58.1	65.3	5.8	4.4	57.3	60.1	6.9	10.6
S	15.6	26.7	17.2	19.1	10.4	25.9	48.4	38.7	11.0	30.4	15.8	20.1
G_2/M	24.6	6.8	19.1	11.7	27.2	5.7	36.9	41.6	28.8	7.3	32.2	27.5
MCF-7 cells												
Sub-G_1	4.2	17.5	3.9	5.8	5.3	11.1	2.9	16.8	5.1	10.3	3.6	2.5
G_1	57.6	53.4	28.8	63.7	55.8	61.3	22.3	60.6	58.8	57.2	27.9	25.8
S	16.8	26.9	4.7	21.4	19.1	22.1	21.2	13.8	16.4	28.6	5.0	20.4
G_2/M	21.4	2.2	62.6	9.1	25.1	5.5	53.6	8.8	19.7	3.9	63.5	51.3

early S phase, in which cells are sensitive to cisplatin (20). This may explain the synergistic effects of sequential exposure to pemetrexed followed by cisplatin. On the contrary, one agent may reduce the cytotoxicity of the other agent by preventing cells from entering the specific phase in which the cells are most cytotoxic to the other agent. It has been shown that cisplatin elicits cytotoxic effects by blocking cells in G_2/M phase (20), while pemetrexed does by blocking cells in S phase (21). Indeed, simultaneous exposure to pemetrexed and cisplatin produced antagonistic effects, which were caused by the cancellation of cisplatin-induced G_2/M arrest by coexisting pemetrexed in PA1 and MCF7 cells. This was also the case with sequential exposure with cisplatin first followed by pemetrexed.

Our findings suggest that the sequential administration of pemetrexed followed by cisplatin may be the optimal schedule for these combinations. For example, administrations of pemetrexed on day 1 and cisplatin on day 2 would be worthy of clinical investigations. The simultaneous administration of pemetrexed and cisplatin and the sequential administration of cisplatin followed by pemetrexed may be inadequate. However, it must be noted that there are a number of difficulties in the translation of results from in vitro models to clinical therapy. The drug metabolism and pharmacokinetics under in vivo and in vitro conditions are different. Clinical outcome includes both the antitumor effects and normal tissue toxicity that results from a variable drug exposure, whereas in vitro models represent only antitumor effects at a constant drug exposure.

Teicher et al. studied the combination of pemetrexed with cisplatin in vivo against EMT-6 murine mammary carcinoma by a tumor cell survival assay (26). They observed that pemetrexed administered four times over 48 h with cisplatin administered with the third dose of pemetrexed produced an additive or more than additive tumor response. Teicher et al. further studied the combination of pemetrexed with cisplatin in human tumor xenografts (27). Administration of pemetrexed (days 7–11, days 14–18) along with cisplatin (day 7) produced greater-than-additive effects for human lung cancer H460 and Calu-6 tumor growth delay. Because experimental systems, schedules of drug administrations, and evaluating methods for synergism are different, it is difficult to compare their findings and ours.

A clinical and pharmacokinetic phase I study of pemetrexed in combination with cisplatin has been reported by Thordtmann et al. (15). They observed that this combination was clinically active and simultaneous administration of both agents on day on 1 (pemetrexed intravenously over 10 min and cisplatin over 2 h) every 21 days was less toxic than a sequential administration of pemetrexed on day 1 and cisplatin on day 2. They recommended the simultaneous administration of pemetrexed at 500 mg/m^2 plus cisplatin at 75 mg/m^2 on day 1 every 21 days for this combination. Phase II and III studies of the same schedules have been started for this combination and encouraging results have been obtained so far (16–18).

Our in vitro findings are not contradictory to clinical findings. In our study, simultaneous exposure to pemetrexed and cisplatin produced additive effects in WiDr cells and antagonistic effects in A549, MCF7, andPA1 cells. Most data points fell in the area of sudadditivity in MCF7 and PA1 cells, suggesting that the combination is superior to each drug alone but "sub-optimal." The simultaneous administration of pemetrexed and cisplatin was less toxic than the sequential administration, probably due to antagonistic interaction in the simultaneous exposure. Our isobologram shows that the doses of both agents in the pemetrexed–cisplatin sequence required

for IC_{80} or IC_{50} levels were much less (40–90%) than of those in simultaneous exposure (Fig. 3). Pemetrexed at 500 mg/m^2 and cisplatin at 75 mg/m^2, the optimal dose for the simultaneous administration, would be overdosed for the sequential administration of pemetrexed followed by cisplatin, which produced synergistic effects.

In conclusion, the present findings show that the interaction of pemetrexed and cisplatin is definitely schedule dependent. Sequential exposure to pemetrexed followed by cisplatin produced synergistic effects, whereas simultaneous exposure to the two agents and sequential exposure to cisplatin followed by pemetrexed produced antagonistic effects. These findings suggest that the optimal schedule of pemetrexed in combination with cisplatin at the cellular level is the sequential administration of pemetrexed followed by cisplatin. Although the simultaneous administration of pemetrexed and cisplatin on day 1 is more convenient and less toxic for patients than the sequential administration of pemetrexed on day 1 and cisplatin on day 2, the former schedule may be suboptimal and may not improve the clinical efficacy to "originally expected" level for this combination. It would be important to conduct dose-finding clinical trials in sequential administration of pemetrexed and cisplatin.

ACKNOWLEDGMENTS: This work was supported in part by a Grant-in-Aid for Cancer Research (11-8) from the Ministry of Health and Welfare and by a Grant-in-Aid for Research on the Second-Term Comprehensive 10-Year Strategy for Cancer Control from the Ministry of Health and Welfare of Japan.

REFERENCES

1. Taylor, E. C.; Kuhnt, D.; Shih, C.; Rinzel, S. M.; Grindey, G. B.; Barredo, J.; Jannatipour, M.; Moran, R. G. A dideazatetrahydrofolate analogue lacking a chiral center at C-6 N-[4-[2-(2-amino-34-dihydro-4-oxo-7H-pyrrolo[23-d]pyrimidin-5- yl)ethyl]benzoyl]-L-glutamic acid is an inhibitor of thymidylate synthase. J. Med. Chem. 35:4450–4454; 1992.
2. Habeck, L. L.; Mendelsohn, L. G.; Shih, C.; Taylor, E. C.; Colman, P. D.; Gossett, L. S.; Leitner, T. A.; Schultz, R. M.; Andis, S. L.; Moran, R. G. Substrate specificity of mammalian folypolyglutamate synthetase for 510-dideazatetrahydrofolate analogs. Mol. Pharmacol. 48: 326–333; 1995.
3. Shih, C.; Habeck, L. L.; Mendelsohn, L. G.; Chen, V. J.; Schultz, R. M. Multiple folate enzyme inhibition: Mechanism of a novel pyrrolopyrimidine-based antifolate LY231514 (MTA). Adv. Enzyme Regul. 38:135–152; 1998.
4. Shih, C.; Thornton, D. E. Preclinical pharmacology studies and the clinical development of a novelmultitargeted antifolate MTA (LY231514) In: Jackman, A. L., ed. Anticancer drug development guide: Antifolate drugs in cancer therapy. Totowa, NJ: Humana Press; 1998:183–201.
5. McDonald, A. C.; Vasey, P. A.; Adams, L.; Walling, J.; Woodworth, J. R.; Abrahams, T.; McCarthy, S.; Bailey, N. P.; Siddiqui, N.; Lind, M. J.; Calvert, A. H.; Twelves, C. J.; Cassidy, J.; Kaye, S. B. A phase I and pharmacokinetic study of LY231514 the multitargeted antifolate. Clin. Cancer Res. 4:605–610; 1998.
6. Rinaldi, D. A. Overview of phase I trials of multitargeted antifolate (MTA LY231514). Semin. Oncol. 26(Suppl. 6): 82–88; 1999.
7. Rusthoven, J. J.; Eisenhauer, E.; Butts, C.; Gregg, R.; Dancey, J.; Fisher, B.; Iglesias, J. Multitargeted antifolate LY231514 as first-line chemotherapy for patients with advanced non-small-cell lung cancer: A phase II study. National Cancer Institute of Canada Clinical Trials Group. J. Clin. Oncol. 17:1194–1199; 1999.
8. John, W.; Picus, J.; Blanke, C. D.; Clark, J. W.; Schulman, L. N.; Rowinsky, E. K.; Thornton, D. E.; Loehrer, P. J. Activity of multitargeted antifolate (pemetrexed disodium LY231514) in patients with advanced colorectal carcinoma: Results from a phase II study. Cancer 88:1807–1813; 2000.
9. Hanauske, A. R.; Chen, V.; Paoletti, P.; Niyikiza, C. Pemetrexed disodium: A novel antifolate clinically active against multiple solid tumors. Oncologist 6:363–373; 2001.
10. Pivot, X.; Raymond, E.; Laguerre, B.; Degardin, M.; Cals, L.; Armand, J. P.; Lefebvre, J. L.; Gedouin, D.; Ripoche, V.; Kayitalire, L.; Niyikiza, C.; Johnson, R.; Latz, J.; Schneider, M. Pemetrexed disodium in recurrent locally advanced or metastatic squamous cell carcinoma of the head and neck. Br. J. Cancer 85:649–655; 2001.
11. Shepherd, F. A. Pemetrexed in the treatment of non-small cell lung cancer. Semin. Oncol. 29(Suppl. 18):43–48; 2002.
12. Calvert, H. Pemetrexed (Alimta): A promising new agent for the treatment of breast cancer. Semin. Oncol. 30 (Suppl. 3):2–5; 2003.
13. Scagliotti, G. V.; Shin, D. M.; Kindler, H. L.; Scagliotti, G. V.; Shin, D. M.; Kindler, H. L.; Vasconcelles, M. J.; Keppler, U.; Manegold, C.; Burris, H.; Gatzemeier, U.; Blatter, J.; Symanowski, J. T.; Rusthoven, J. J. Phase II study of pemetrexed with and without folic acid and vitamin B12 as front-line therapy in malignant therapy in malignant pleural mesothelioma. J. Clin. Oncol. 21:1556–1561; 2003.
14. Hanna, N.; Shepherd, F. A.; Fossella, F. V.; Pereira, J. R.; De Marinis, F.; von Pawel, J.; Gatzemeier, U.; Tsao, T. C.; Pless, M.; Muller, T.; Lim, H. L.; Desch, C.; Szondy, K.; Gervais, R.; Shaharyar; Manegold, C.; Paul, S.; Paoletti, P.; Einhorn, L.; Bunn, Jr., P. A. Randomized phase III trial of pemetrexed versus docetaxel in patients with non-small-cell lung cancer previously treated with chemotherapy. J. Clin. Oncol. 22:1589–1597; 2004.
15. Thodtmann, R.; Depenbrock, H.; Dumez, H.; Blatter, J.; Johnson, R. D.; van Oosterom, A.; Hanauske, A. R. Clinical and pharmacokinetic phase I study of multitargeted antifolate (LY231514) in combination with cisplatin. J. Clin. Oncol. 17:3009–3016; 1999.
16. Manegold, C.; Gatzemeier, U.; von Pawel, J.; Pirker, R.; Malayeri, R.; Blatter, J.; Krejcy, K. Front-line treatment of advanced non-small-cell lung cancer with MTA (LY231514 pemetrexed disodium ALIMTA) and cisplatin: A multicenter phase II trial. Ann. Oncol. 11:435–440; 2000.
17. Shepherd, F. A.; Dancey, J.; Arnold, A.; Neville, A.; Rusthoven, J.; Johnson, R. D.; Fisher, B.; Eisenhauer, E. Phase II study of pemetrexed disodium a multitargeted antifolate and cisplatin as first-line therapy in patients with advanced non small cell lung carcinoma: A study

of the National Cancer Institute of Canada Clinical Trials Group. Cancer 92:595–600; 2001.
18. Vogelzang, N. J.; Rusthoven, J. J.; Symanowski, J.; Denham, C.; Kaukel, E.; Ruffie, P.; Gatzemeier, U.; Boyer, M.; Emri, S.; Manegold, C.; Niyikiza, C.; Paoletti, P. Phase III study of pemetrexed in combination with cisplatin versus cisplatin alone in patients with malignant pleural mesothelioma. J. Clin. Oncol. 21:2636–2644; 2003.
19. Scagliotti, G. V.; Kortsik, C.; Dark, G. G.; Price, A.; Manegold, C.; Rosell, R.; O'Brien, M.; Peterson, P. M.; Castellano, D.; Selvaggi, G.; Novello, S.; Blatter, J.; Kayitalire, L.; Crino, L.; Paz-Ares, L.; Go, R. S. Pemetrexed combined with oxaliplatin or carboplatin as first-line treatment in advanced non-small cell lung cancer: A multicenter, randomized, phase II trial. Clin. Cancer Res. 11(2 Pt. 1):690–696; 2005.
20. Adjei, A. A. Review of the comparative pharmacology and clinical activity of cisplatin and carboplatin. J. Clin. Oncol. 17:409–422; 1999.
21. Jackel, M.; Kopf-Maier, P. Influence of cisplatin on cell-cycle progression in xenografted human head and neck carcinomas. Cancer Chemother. Pharmacol. 27:464–471; 1991.
22. Tonkinson, J. L.; Marder, P.; Andis, S. L.; Schultz, R. M.; Gossett, L. S.; Shih, C.; Mendelsohn, L. G. Cell cycle effects of antifolate antimetabolites: Implications for cytotoxicity and cytostasis. Cancer Chemother. Pharmacol. 39: 521–531; 1997.
23. Tonkinson, J. L.; Worzalla, J. F.; Teng, C. H.; Mendelsohn, L. G. Cell cycle modulation by a multitargeted antifolate, LY231514, increases the cytotoxicity and antitumor activity of gemcitabine in HT29 colon carcinoma. Cancer Res. 59:3671–3676; 1999.
24. Schultz, R. M.; Dempsey, J. A. Sequence dependence of Alimta (LY231514, MTA) combined with doxorubicin in ZR-75-1 human breast carcinoma cells. Anticancer Res. 21:3209–3214; 2001.
25. Kano, Y.; Akutsu, M.; Tsunoda, S.; Izumi, T.; Mori, K.; Fujii, H.; Yazawa, Y.; Mano, H.; Furukawa, Y. Schedule-dependent synergism and antagonism between pemetrexed and paclitaxel in human carcinoma cell lines in vitro. Cancer Chemother. Pharmacol. 54:505–513; 2004.
26. Teicher, B. A.; Alvarez, E.; Liu, P.; Lu, K.; Menon, K.; Dempsey, J.; Schultz, R. M. MTA (LY231514) in combination treatment regimens using human tumor xenografts and the EMT-6 murine mammary carcinoma. Semin. Oncol. 28:55–62; 1999.
27. Teicher, B. A.; Chen, V.; Shih, C.; Menon, K.; Forler, P. A.; Phares, V. G.; Amsrud, T. Treatment regimens including themultitargeted antifolate LY231514 in human tumor xenografts. Clin. Cancer Res. 6:1016–1023; 2000.
28. Kano, Y.; Sakamoto, S.; Kasahara, T.; Akutsu, M.; Inoue, Y.; Miura, Y. In vitro effects of amsacrine in combination with other anticancer agents. Leukemia Res. 15:1059–1064; 1991.
29. Steel, G. G.; Peckham, M. J. Exploitable mechanisms in combined radiotherapy-chemotherapy: the concept of additivity. Int. J. Radiat. Oncol. Biol. Phys. 5:85–91; 1979.
30. Kano, Y.; Ohnuma, T.; Okano, T.; Holland, J. F. Effects of vincristine in combination with methotrexate and other antitumor agents in human acute lymphoblastic leukemia cells in culture. Cancer Res. 48:351–356; 1988.
31. Kano, Y.; Akutsu, M.; Tsunoda, S.; Mano, H.; Sato, Y.; Honma, Y.; Furukawa, Y. In vitro cytotoxic effects of a tyrosine kinase inhibitor STI571 in combination with commonly used antileukemic agents. Blood 97:1999–2007; 2001.
32. Kano, Y.; Akutsu, M.; Tsunoda, S.; Suzuki, K.; Adachi, K. In vitro schedule-dependent interaction between paclitaxel and SN-38 (the active metabolite of irinotecan) in human carcinoma cell lines. Cancer Chemother. Pharmacol. 42:91–98; 1998.
33. Furukawa, Y.; Iwase, S.; Kikuchi, J.; Nakamura, M.; Terui, Y.; Yamada, H.; Kano, Y.; Matsuda, M. Phosphorylation of bcl-2 protein by cdc2 Kinase during G2/M phases and its role in cell cycle regulation. J. Biol. Chem. 275:21661–21667; 2000.

Clinical Study

Chemotherapy

Chemotherapy 2005;51:120–125
DOI: 10.1159/000085619

Received: May 15, 2004
Accepted after revision: November 19, 2004
Published online: May 9, 2005

A Phase II Study of Docetaxel and Infusional Cisplatin in Advanced Non-Small-Cell Lung Cancer

Kiyoshi Mori Yukari Kamiyama Tetsuro Kondo Yasuhiko Kano
Tetsuro Kodama

Department of Thoracic Diseases, Tochigi Cancer Center, Yonan, Utsunomiya, Japan

Key Words
Non-small-cell lung cancer · Chemotherapy · Cisplatin · Docetaxel · Infusion, continuous

Abstract
Background: To evaluate the efficacy and safety of combination chemotherapy of cisplatin (5-day continuous infusion) and docetaxel for the treatment of previously untreated patients with advanced non-small-cell lung cancer (NSCLC). ***Materials and Methods:*** Eligible patients had an ECOG performance status of 0–2 with measurable NSCLC. Patients received continuous infusion cisplatin 20 mg/m^2/day on 5 days and bolus docetaxel 60 mg/m^2/day (day 1; PiD therapy) at a 4-week interval. ***Results:*** Forty-three patients were enrolled. The mean number of cycles administered per patient was 2, and ranged from 1 to 4. The response rate was 49% (95% confidence interval, 33.9–63.8%). The median survival time was 47 weeks and the 1-year survival rate was 47%. The major toxic effects were grade 3 or 4, neutropenia (88%), leukopenia (81%), thrombocytopenia (14%) and anemia (42%). There were no treatment-related deaths. ***Conclusion:*** PiD therapy was a well-tolerated and active regimen for patients with advanced NSCLC. The major toxicity was neutropenia.

Introduction

Unresectable non-small-cell lung cancer (NSCLC) is known to have an extremely poor prognosis, and its standard treatment remains to be established. The most common chemotherapy for NSCLC is a combination treatment consisting of 2 or 3 drugs including cisplatin (CDDP) as a key drug. The combination treatments have response rates of 30–50%, and have been proven to prolong survival time in clinical stages III [1] and IV [2, 3]; however, the response is only limited.

In recent years, new anticancer drugs have been developed and used for the treatment of NSCLC. Docetaxel is a new hemisynthetic anticancer agent originating from its precursor, 10-deacytylbaccatin III, extracted from the needle leaves of the European yew tree, *Taxus baccata* L. Docetaxel affects microtubules, and shows its cytotoxicity by prematurely stabilizing mitotic microtubules. In phase II clinical studies for the treatment of NSCLC carried out in Europe and the USA, docetaxel showed a response rate of about 30% in previously untreated patients with a better survival time [4, 5]. A major side effect of docetaxel is dose-dependent edema that is proportional to bone marrow suppression. Since hypersensitivity is particularly limiting, it is worth noting that docetaxel can be given by intravenous infusion in a short period of time without any pretreatment.

KARGER
Fax +41 61 306 12 34
E-Mail karger@karger.ch
www.karger.com

0009–3157/05/0513–0120$22.00/0

Accessible online at:
www.karger.com/che

Kiyoshi Mori
Department of Thoracic Diseases, Tochigi Cancer Center
4-9-13, Yonan
Utsunomiya, Tochigi 320-0834 (Japan)
Tel. +81 28 658 5151, Fax +81 28 658 5669, E-Mail kmori@tcc.pref.tochigi.jp

In the Japan phase I study, dose-limiting toxicity of docetaxel was found to be leukopenia (neutropenia), and its recommended dose was set at 60 mg/m^2 [6]. In the multicenter phase II clinical study for the treatment of NSCLC carried out in Japan, a response rate of 19% was shown in untreated patients with predominant toxicities of leukopenia and neutropenia [7].

Currently, cisplatin is the active agent for treating NSCLC, and combination chemotherapy consisting of 2 or 3 drugs based on CDDP is a major strategy [8]. CDDP can be administered by short-term intravenous infusion, a divided dosage method, continuous administration, and other methods [9, 10]. CDDP cytotoxicity is enhanced by prolonged exposure to low doses of this drug in in vitro studies [11, 12]. Belliveau et al. [13] reported that the area under the concentration-time curve (AUC) achieved for non-protein-bound CDDP was twice as high after 5-day continuous infusion than that observed when an equivalent dose of CDDP was given by short-term bolus infusion. These findings suggest that continuous infusion of CDDP might improve the therapeutic efficacy as compared with that resulting from conventional short-term bolus infusion. However, compared with short-term intravenous infusion, 5-day continuous infusion makes inpatient hospitalization for at least 5 days necessary, and the duration of confinement for the purpose of infusion is lengthy and therefore onerous for the patient. The efficacy and safety of a continuous infusion lasting 5 days (24 h a day) were confirmed in our facility and some other facilities [10, 14–16]. In addition, combination chemotherapy of infusional CDDP with vindesine or CPT-11 was found to have high response rates in treating NSCLC [17, 18].

Cisplatin and docetaxel show nonsynergistic and additive effects in vitro, no cross-resistance and have a relatively nonoverlapping toxicity profile [19]. Therefore, the development of docetaxel in combination with cisplatin is warranted. We conducted a phase II study of docetaxel and infusional cisplatin, in patients with previously untreated advanced NSCLC, and evaluated antitumor activity and the safety of this therapy.

Patients and Methods

Patient Selection

All patients with histologically or cytologically confirmed advanced NSCLC were eligible for this phase II trial. The subjects of this study were patients in clinical stage IV or in stage III with unresectable disease or in whom radiotherapy with curative intent is not possible. Patients with unresectable disease or in whom radiotherapy with curative intent is not possible include those with pleural effusion and dissemination, those with intrapulmonary metastasis within the ipsilateral lobe, those in whom the irradiation field exceeds one half of one lung, those with metastasis to the contralateral hilar lymph nodes, and those with reduced lung function. None of the patients had received prior therapy. Other eligibility criteria included an expected survival of 12 weeks, age ≤75 years, Eastern Cooperative Oncology Group performance score of 0–2, measurable lesions, adequate hematological function (WBC ≥4,000/mm^3, platelet count ≥100,000/mm^3, hemoglobin ≥10 g/dl), renal function (serum creatinine ≤1.5 mg/dl, creatinine clearance ≥60 ml/min), and hepatic function (total serum bilirubin ≤1.5 mg/dl, glutamic oxaloacetic transaminase and glutamic pyruvic transaminase less than twice the normal range). The ethical committee of the Tochigi Cancer Center approved the protocols. Written informed consent was obtained in every case stating that the patient was aware of the investigational nature of this treatment regimen. Pretreatment evaluation included medical history, physical examination, complete blood count, bone marrow examination, serum biochemical analyses, chest roentgenogram, electrocardiogram, and urinalysis. All patients underwent a radionuclide bone scan, and computerized tomography of the brain, thorax and abdomen. Complete blood count, biochemical tests, serum electrolytes, urinalysis, and chest roentgenograms were obtained weekly during this phase II trial. Tests of measurable disease parameters such as computerized tomography were repeated every 4 weeks. Staging was according to the 4th edition of the UICC TNM classification.

Treatment

All patients were admitted to the Tochigi Cancer Center Hospital during this trial. The anticancer drug regimen consisted of a combined administration of docetaxel plus infusional cisplatin. Docetaxel was supplied, in concentrated form, in a sterile vial that contained 80 mg of the drug in 2 ml of polysorbate 80. Docetaxel (Taxotere; Aventis) 60 mg/m^2 was diluted in 250 ml of 5% glucose, and was infused over a 1-hour period on day 1. Three hours after completion of the docetaxel infusion, 20 mg/m^2 of cisplatin was given daily for 5 days by continuous intravenous infusion. One third of the daily dose was administered every 8 h dissolved in 800 ml of physiological saline [14]. The course was repeated every 4 weeks. Antiemetic drugs used were granisetron (3 mg/body/day, bolus infusion for 5 days), metoclopramide (3 mg/kg/day, continuous infusion for 5 days), methylprednisolone (125 mg bolus infusion every 8 h, days 1–5), diphenhydramine (30 mg orally, days 1–7) and alprazolam (1.2 mg orally, days 1–7) [15, 16]. In the first course, no routine premedication was given for hypersensitivity reactions or fluid retention. The reason for this was that the incidence of these events was low at the dose of docetaxel (60 mg/m^2) administered in the present study [7]. However, if hypersensitivity reactions or fluid retention occurred, premedications such as corticosteroids or antiallergic agents were allowed in the subsequent courses. Recombinant human granulocyte colony-stimulating factor was administered when leukopenia/neutropenia of grade 4 occurred.

Patients were treated with at least two cycles of therapy unless disease progression or unacceptable toxicity was encountered or the patients did not wish to continue. Patients who experienced grade 4 leukopenia or neutropenia that lasted for 3 or more days, or who experienced grade 4 thrombocytopenia or reversible grade 2 neurotoxicity or grade 3 liver dysfunction, received reduced doses of

both docetaxel and cisplatin (75% of the previous dose) for the next cycle. Patients who experienced stomatitis of grade 3 or more or renal dysfunction of grade 2 or more received a reduced dose of cisplatin (75% of the previous dose) for the next cycle. If neurotoxicity of grade 3 or more occurred, treatment was stopped. Subsequent courses of chemotherapy were started after day 28 when the leukocyte count was 4,000/mm^3 or more, the neutrophil count was 2,000/mm^3 or more, the platelet count was 100,000/mm^3 or more, serum creatinine was less than the upper limit of the normal range, creatinine clearance was 60 ml/min or more, GOT and GPT were less than twice the upper limit of the normal range, and neurotoxicity was grade 1 or less. If these variables did not return to adequate levels by the first day of the next course of chemotherapy, treatment was withheld until full recovery. If more than 6 weeks passed from the time of the last treatment before these criteria were satisfied, the patient was taken off the study, but still included in the analysis. In the case of stable or progressive disease after two courses of treatment, subsequent therapy was left to the discretion of the physician in charge of the patient.

Assessment of Response to Treatment and Toxicity

The response to treatment was evaluated with WHO criteria. The criteria for response were as follows. Complete response was defined as the complete disappearance of all evidence of tumor for at least 4 weeks. Partial response was defined as a $\geq 50\%$ reduction in the sum of the product of the two greatest perpendicular diameters of all indicator lesions for at least 4 weeks and no appearance of new lesions or progression of any lesion. Progressive disease was defined as a $\geq 25\%$ increase in the tumor area or the appearance of new lesions. All other circumstances were classified as no change. Toxicity was graded according to the common toxicity criteria (version 2).

Statistical Analyses

The primary end point was the objective response rate. The duration of each response was defined as the number of days from the documentation of the response until tumor progression. Survival curves from registration until death were generated by the method of Kaplan and Meier. We chose a 40% response rate as a desirable target level, and a 20% response rate as undesirable. The study design had the power to detect a response of greater than 90%, with less than 5% error. Therefore, we needed 23 assessable patients in first stage and 20 in second stage, according to the mini-max design of Simon. We decided to stop the study if fewer than 5 patients responded in the first stage.

Results

Patient Characteristics

Forty-three patients were enrolled in this study from July 1997 to June 1999 and received 105 cycles of the regimen. Table 1 shows the patient characteristics. There were 14 women and 29 men with a median age of 61 years (range 34–75). One patient had stage IIIA, 7 patients stage IIIB, and 35 patients stage IV disease. In stage IIIA, 1 patient classified as c-T3N2M0 had lung cancer with a bulky tumor (10 cm), associated with extranodal and N2 involvement. Among the 7 stage IIIB patients, there were three T4 cases in which pleural effusion and pleural dissemination were present, two T4 cases of intrapulmonary metastasis in the ipsilateral lobe, and two T4N3 cases with mediastinal infiltration and supraclavicular fossa lymph node metastasis.

Table 1. Patient characteristics

Patients	43
Sex (M/F)	29/14
Age[1], years	61 (34–75)
Performance status: 0/1/2	9/30/4
Stage: IIIA/IIIB/IV	1/7/35
Histology: Ad/Sq/Other	27/14/2

Ad = Adenocarcinoma; Sq = squamous cell carcinoma.

[1]Value represents median with the range given in parentheses.

Treatments Administered

The mean number of cycles administered per patient was 2, and ranged from 1 to 4. In 99 of 105 cycles (94%), PiD was administered at 4-week intervals. In 5 of 6 cycles, in which cisplatin could not be administered at a 4-week interval, it was given a week later. As for the remaining cycle, it was administered 6 weeks later. The reason for the delay of the administration was the patient's request for 1 cycle and neutropenia in 5 cycles. Dosage was reduced in 7 cycles (7%). Reductions in dosage of docetaxel and cisplatin were made, respectively, in 6 cycles (6%) and 7 cycles (7%). The former reduction was made because 6 cycles showed neutropenia grade 4, and the latter reduction was made because 5 cycles showed neutropenia grade 4, and 1 cycle showed both neutropenia grade 4 and creatinine grade 3, and 1 cycle showed creatinine grade 2.

Response to Treatment and Survival

The response rate was 49% (95% confidence interval, CI, 33.9–63.8%); a complete response was observed in 1 and partial response in 20 patients (table 2). The median duration of the response was 39.2 weeks (range 5–147 weeks). The median survival time was 47 weeks (95% CI, 6–152 weeks) and the 1-year survival rate was 47% (fig. 1). Two patients are still alive.

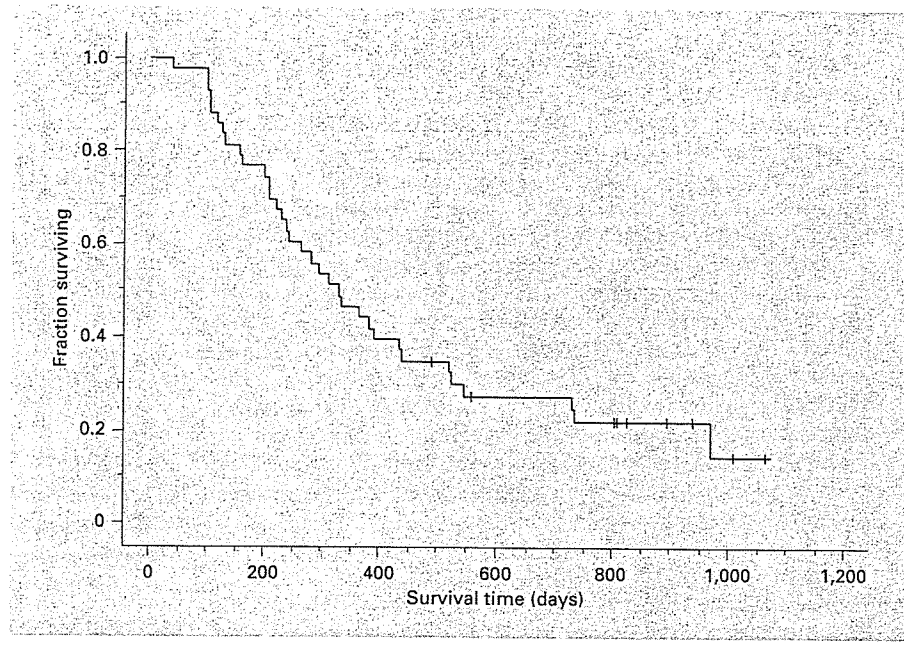

Fig. 1. Kaplan-Meier estimated overall survival curves. Median survival time was 47 weeks; 1-year survival rate was 47%.

Table 2. Chemotherapeutic evaluation (n = 43)

Cycles[1]	2 (1–4)
Response: CR/PR/NC/PD	1/20/20/2
Response rate, %	49
Response duration, weeks	
Average	39.2
Range	5–147
1-year survival rate, %	47

CR = Complete response; PR = partial response; NC = no change; PD = progressive disease.

[1]Value represents average with the range in parentheses.

Table 3. Toxicity (n = 43 patients)

	Maximum toxicity terms of CTC grade					Grade ≥3
	0	1	2	3	4	%
Leukopenia	1	1	6	29	6	81
Neutropenia	1	0	4	13	25	88
Anemia	1	6	18	18	–	42
Thrombocytopenia	25	5	7	6	0	14
Creatinine	23	18	1	1	0	2
SGOT/SGPT	30	12	1	0	0	0
Vomiting	5	7	31	0	–	0
Diarrhea	20	16	7	0	0	0
Alopecia	20	22	1	–	–	
Edema	36	6	1	0	–	0
Neuropathy	40	3	0	0	0	0

Figures represent number of patients. CTC = Common toxicity criteria; SGOT = serum glutamic oxaloacetic transaminase; SGPT = serum glutamic pyruvic transaminase.

Toxicity

Table 3 shows the types and grades of toxicities resulting from the treatment, using the common toxicity criteria. All 43 patients could be evaluated for toxic reactions. The major toxicity was myelosuppression. Leukopenia <2,000/mm^3 (grade 3 or 4) was observed in 35 patients (81%), of whom 6 patients showed grade 4. Neutropenia <1,000/mm^3 (grade 3 or 4) was observed in 38 patients (88%), of whom 25 patients showed grade 4. Eight patients developed febrile neutropenia. Thrombocytopenia <5 × 10^4/mm^3 (grade 3 or 4) was observed in 6 patients (14%), and a hemoglobin nadir (grade 3) in 18 patients (42%). There were no episodes of bleeding or fluid overload.

Vomiting grade ≥2 occurred in 31 patients (72%). Diarrhea grade ≥2 was observed in 7 patients (16%). Grade 1 or 2 alopecia and edema were observed in 23 and 7 patients, respectively. In the first cycle, creatinine showed grade ≥2 in 2 patients, resulting in transient rises. In the following cycle, the creatinine level was kept at grade 1 by reducing the dosage of cisplatin. Grade 1 or 2 skin rash was observed in 3 patients. Finally, there were no treatment-related deaths.

Discussion

Cisplatin is one of the key drugs for the treatment of NSCLC. Its high response rate of 40% and safety when it was given alone by continuous infusion over 5 days [14] are confirmed.

Docetaxel is also an active agent to treat NSCLC, and docetaxel of 60 mg/m^2/day (day 1), a recommended dose in Japan, showed a response rate of 19% [7]. Docetaxel has no cross-resistance with cisplatin, and in clinical practice, docetaxel was effective in some patients who were resistant to cisplatin [19]. In addition, additive effects are confirmed between cisplatin and docetaxel, and major side effects of the two drugs are different.

This was a phase II study to determine the usefulness and safety of combination chemotherapy of cisplatin (5-day continuous infusion) and docetaxel for the treatment of advanced NSCLC. The response rate in this study was 49%, which is higher than with docetaxel alone. In comparison with other combination therapies, response rates were 39–42% for cisplatin (bolus) and docetaxel [20, 21], and 58.5% for cisplatin (infusion) and irinotecan with G-CSF. In combination with cisplatin (bolus) and newly developed anticancer agents, the response rates were 44% with paclitaxel [22], 31% with gemcitabine [23], and 26% with vinorelbine [24]. Although these studies differed as regards patients' backgrounds, generally, combination therapies showed better response rates than docetaxel alone.

In our study, side effects predominantly involved hematological toxicity (leukopenia, neutropenia, and anemia). Fever associated with neutropenia was observed in 8 (23%) of 43 patients, and they were treated by administering antibiotics. Hematological toxicities were similar to those in other combination therapies [20, 21]. Nonhematological toxicities were mild, with only 1 patient showing an increased creatinine level of grade 3. The increase was transient, and soon returned to normal. Peripheral edema was observed in only 16%, which was markedly lower than the 24–46% found in other studies [5, 25, 26]. When accumulated doses of docetaxel exceeded 500 mg/m^2, the incidence of edema increased, and at a dose of 85 mg/m^2 or less, eruption was not observed [27]. The dosage was 60 mg/m^2 in our study, and no patients received 500 mg/m^2. There were no side effects concerning hypersensitivity or treatment-related deaths.

We carried out a phase II study of combination treatment of cisplatin (5-day continuous infusion) and docetaxel in 43 patients with NSCLC. The response rate was 49%, and median survival time was 47 weeks. A major side effect was neutropenia. A combination treatment of infusional cisplatin and docetaxel is a tolerable and active regimen for patients with advanced NSCLC. It is to be recommended as a candidate regimen in planning a phase III clinical study in advanced NSCLC, and this regimen will ultimately be evaluated in a phase III clinical study.

Acknowledgement

This work was supported in part by a grant-in-aid for cancer research from the Ministry of Health, Labour and Welfare (Tokyo, Japan), and by the Second Term Comprehensive 10-Year Strategy for Cancer Control.

References

1 Dillman RO, Seagren SL, Propert KJ, et al: A randomized trial of induction chemotherapy plus high-dose radiation versus radiation alone in stage III non-small-cell lung cancer. N Engl J Med 1990;323:940–945.
2 Rapp E, Pater JL, Willan A, et al: Chemotherapy can prolong survival in patients with advanced non-small cell lung cancer – Report of a Canadian multicenter randomized trial. J Clin Oncol 1988;6:633–641.
3 Pronzato P, Landucci M, Vaira A, Bertelli G: Carboplatin and etoposide as outpatient treatment of advanced non-small-cell lung cancer. Chemotherapy 1994;40:144–148.
4 Fossella FV, Lee JS, Murphy WK, et al: Phase II study of docetaxel for recurrent or metastatic non-small-cell lung cancer. J Clin Oncol 1994;12:1238–1244.
5 Francis PA, Rigas JR, Kris MG, et al: Phase II trial of docetaxel in patients with stage III and IV non-small-cell lung cancer. J Clin Oncol 1994;12:1232–1237.
6 Taguchi T, Furuse K, Niitani H, et al: Phase I clinical trial of RP 56976 (docetaxel), a new anticancer drug (in Japanese). Jpn J Cancer Chemother 1994;21:1997–2005.
7 Kunitoh H, Watanabe K, Onoshi T, et al: Phase II trial of docetaxel in previously untreated advanced non-small-cell lung cancer: A Japanese cooperative study. J Clin Oncol 1996; 14:1649–1655.

8 Ruckdeschel JC, Finkelstein DM, Mason BA, et al: Chemotherapy for metastatic non-small-cell bronchogenic carcinoma: EST 2575, generation V-A randomized comparison of four cisplatin-containing regimens. J Clin Oncol 1985;3:72–79.
9 Nakanishi Y, Takayama K, Wataya H, et al: Phase I study of weekly irinotecan combined with weekly cisplatin in patients with advanced solid tumors. Chemotherapy 2002;48:205–210.
10 Forastiere AA, Belliveau JF, Goren MP, et al: Pharmacokinetic and toxicity evaluation of five-day continuous infusion versus intermittent bolus *cis*-diamminedichloroplatinum (II) in head and neck cancer patients. Cancer Res 1988;48:3869–3874.
11 Drewinko B, Brown BW, Gottlieb JA: The effect of *cis*-diamminedichloroplatinum (II) on cultured human lymphoma cells and its therapeutic implications. Cancer Res 1973;33:3091–3095.
12 Matsushima Y, Kanzawa F, Hoshi A, et al: Time-schedule dependency of the inhibiting activity of various anticancer drugs in the clonogenic assay. Cancer Chemother Pharmacol 1985;14:104–107.
13 Belliveau JF, Posner MR, Ferrari L, et al: Cisplatin administered as a continuous 5-day infusion: Plasma platinum levels and urinary platinum excretion. Cancer Treat Rep 1986;70:1215–1217.
14 Saito Y, Mori K, Tominaga K, et al: Phase II study of 5-day continuous infusion of *cis*-diamminedichloroplatinum (II) in the treatment of non-small-cell lung cancer. Cancer Chemother Pharmacol 1990;26:389–392.
15 Mori K, Saito Y, Tominaga K, Yokoi K, Miyazawa N: Comparison of continuous and intermittent bolus infusions of metoclopramide during 5-day continuous intravenous infusion with cisplatin. Eur J Cancer 1991;27:729–732.
16 Mori K, Saito Y, Tominaga K: Antiemetic efficacy of alprazolam in the combination of metoclopramide plus methylprednisolone. Am J Clin Oncol 1993;16:338–341.
17 Mori K, Saito Y, Tominaga K: Phase II study of cisplatin continuous infusion plus vindesine in the treatment of non-small cell lung cancer. Am J Clin Oncol 1992;15:344–347.
18 Mori K, Machida S, Yoshida T, et al: A phase II study of irinotecan and infusional cisplatin with recombinant human granulocyte colony-stimulating factor support for advanced non-small-cell lung cancer. Cancer Chemother Pharmacol 1999;43:467–470.
19 Fossella FV, Lee JS, Shin DM, et al: Phase II study of docetaxel for advanced or metastatic platinum-refractory non-small-cell lung cancer. J Clin Oncol 1995;13:645–651.
20 Zalcberg J, Millward M, Bishop J, et al: Phase II study of docetaxel and cisplatin in advanced non-small-cell lung cancer. J Clin Oncol 1988;16:1948–1953.
21 Okamoto H, Watanabe K, Segawa Y, et al: Phase II study of docetaxel and cisplatin in patients with previously untreated metastatic non-small-cell lung cancer. Int J Clin Oncol 2000;5:316–322.
22 Giaccone G, Splinter AW, Debruyne C, et al: Randomized study of paclitaxel-cisplatin versus cisplatin-teniposide in patients with advanced non-small-cell lung cancer. J Clin Oncol 1998;16:2133–2141.
23 Sandler AB, Nemunaitis J, Denham C, et al: Phase III trial of gemcitabine plus cisplatin versus cisplatin alone in patients with locally advanced or metastatic non-small-cell lung cancer. J Clin Oncol 2000;18:122–130.
24 Wozniak AJ, Crowley JJ, Balcerzak SP, et al: Randomized trial comparing cisplatin with cisplatin plus vinorelbine in the treatment of advanced non-small-cell lung cancer: A Southwest Oncology Group Study. J Clin Oncol 1998;16:2459–2465.
25 Cerny T, Kaplan S, Pavlidis N, et al: Docetaxel (Taxotere) is active in non-small-cell lung cancer: A phase II trial of the EORTC early clinical trials group (ECTG). Br J Cancer 1994;70:384–387.
26 Miller VA, Rigas JR, Francis PA, et al: Phase II trial of a 75-mg/m^2 dose of docetaxel with prednisone premedication for patients with advanced non-small-cell lung cancer. Cancer 1995;75:968–972.
27 Extra JM, Rousseau F, Bruno R, et al: Phase I and pharmacokinetic study of Taxotere (RP 56976; NSC 628503) given as a short intravenous infusion. Cancer Res 1993;53:1037–1042.

Development of a Novel Computer-Aided Diagnosis System for Automatic Discrimination of Malignant From Benign Solitary Pulmonary Nodules on Thin-Section Dynamic Computed Tomography

Kiyoshi Mori, MD, Noboru Niki, PhD,† Teturo Kondo, MD,* Yukari Kamiyama, MD,* Teturo Kodama, MD,* Yoshiki Kawada, PhD,† and Noriyuki Moriyama, MD‡*

Objectives: As an application of the computer-aided diagnosis of solitary pulmonary nodules (SPNs), 3-dimensional contrast-enhanced (CE) dynamic helical computed tomography (HCT) was performed to evaluate temporal changes in the internal structure of nodules to differentiate between benign nodules (BNs) and malignant nodules (MNs).

Methods: There were 62 SPNs (35 MNs and 27 BNs) included in this study. Scanning (2-mm collimation) was performed before and 2 and 4 minutes after CE dynamic HCT. The CT data were sent to a computer, and the pixels inside the nodule were characterized in terms of 3 parameters (attenuation, shape index, and curvedness value).

Results: Based on the CT data at 4 (MN: 1.81–27.1, BN: −42.8 to −3.29) minutes after CE–dynamic HCT, a score of 0 or higher can be assumed to indicate an MN.

Conclusions: Three-dimensional computer-aided diagnosis of the internal structure of SPNs using CE dynamic HCT was found to be effective for differentiating between BNs and MNs.

Key Words: coin lesion, pulmonary, computer-aided design, lung neoplasms, radiographic image enhancement, tomography, x-ray computed

(*J Comput Assist Tomogr* 2005;29:215–222)

The morphologic imaging diagnosis of solitary pulmonary nodules (SPNs) has been performed based on qualitative findings, mainly in computed tomography (CT) images, identified by diagnosticians when evaluating the characteristics of the nodule's margins, internal structure, and relations to surrounding structures.[1–3] The interpretation of these findings tends to differ, however, depending on the person performing the diagnosis, and diagnostic standards for differentiating between benign nodules (BNs) and malignant nodules (MNs) have yet to be established. The quantitative diagnosis of such lesions has been attempted based on the measurement of attenuation in the nodule. Attenuation has been used for the objective assessment of the internal structure of nodules and for the differential diagnosis of BNs and MNs.[4] There have also been reports on the use of contrast medium to evaluate changes in attenuation in nodules over time to differentiate between BNs and MNs.[5–8] In these studies, however, the attenuation in the nodules was measured in only a few slices. Moreover, because the region of interest (ROI) within the lesion was specified manually, the attenuation obtained showed a large degree of variation in different slices.

The use of helical scanning has facilitated the acquisition of volume data for the entire lesion, making it possible to analyze these image data using a computer.[9–11] In the present study, images of the entire lesion were obtained using contrast-enhanced (CE) dynamic helical computed tomography (HCT), and the changes in the density of the lesion over time were calculated with a computer and quantified in a 3-dimensional (3D) perspective for the differential diagnosis of BNs and MNs.

SUBJECTS AND METHODS

CT Imaging Conditions

Computed tomography images were obtained using an Xpress/SX system (Toshiba Corporation, Tokyo, Japan). The scanning parameters were a patient couch-top movement speed of 2 mm/s, a beam width of 2 mm, a tube voltage of 120 kV, a tube current of 200 mA, 1-second scanning, and an ROI of 200 mm. A total of 100 mL nonionic contrast medium (Iopamiron 300 Syringe; Nihon Schering, Tokyo, Japan) was injected at a rate of 2 mL/s using an autoinjector through a peripheral forearm vein. With the patient placed in the supine position and receiving supplemental oxygen via a nasal cannula (2 L/min), helical scanning covering the entire lesion (40–50 mm) was performed 3 times during breath-holding (before enhancement and 2 and 4 minutes after the start of

Received for publication August 10, 2004; accepted January 3, 2005.
From the *Department of Thoracic Diseases, Tochigi Cancer Center, Tochigi, Japan, †Department of Optical Science, University of Tokushima, Tokushima, Japan, and ‡Department of Radiology, National Cancer Center, Tokyo, Japan.
Supported in part by a grant-in aid for cancer research from the Ministry of Health and Welfare of Japan and the Second-Term Comprehensive 10-Year Strategy for Cancer Control.
Reprints: Kiyoshi Mori, Department of Thoracic Diseases, Tochigi Cancer Center, 4-9-13 Younan, Utsunomiya, Tochigi 320-0834, Japan (e-mail: kmori@tcc.pref.tochigi.jp).

contrast injection). Images were reconstructed at 1-mm intervals using a 180° algorithm.

Evaluation of CT Images

CT Image Processing

The tumor lesion was extracted from the thin-section CT images and then reconstructed to obtain a 3D CT image of the tumor.[9] The density was then calculated by characterizing the pixels inside the extracted nodule in terms of 3 parameters (attenuation, shape index, and curvedness value). Based on the calculated density values within each nodule before enhancement and 2 and 4 minutes after the start of injection, a linear discriminant function score was obtained for each time point.

Extraction of Lesions

After the reconstruction of 3D images from the thin-section CT images, ROIs containing the nodules were extracted from these images (Fig. 1). Using a deformable surface model, the nodules were then extracted from these ROIs.[9,12] In some cases, the nodules were located adjacent to the pleura. In such cases, preprocessing was required for extracting the region of the lung fields to separate the pleura from the nodules.[10] The segmentation of the nodule was based on a thresholding technique and selection of object connected components. In the present study, a method based on the deformable surface model proposed by Caselles et al[12] was used for extracting nodular regions with various density distributions.[10] This approach is based on deforming 3D surfaces, represented by level sets, toward the nodule boundary to be extracted in the 3D images. It automatically handles the changes in the surface topology during deformation. In this method, the nodular region is extracted by placing the initial curved surface within the nodule and then transforming the surface to conform to the margins of the nodule using a formula for the curved surface.[12] In this way, excessive overflow of blood vessels and bronchi relative to the curved surface can be prevented by adjusting the end points for curved surface transformation.[10]

Display and Assessment of Characteristic Values Within the Lesion

The pixels in the ROI, including the nodule, were expressed locally using a combination of 3 parameters: the attenuation, shape index, and curvedness value (Figs. 2, 3).[13,14]

The shape index and curvedness value are defined by the 3D curvature of the curved surface. The shape index ranges from 0 to 1. As the shape index approaches 0, the surface becomes increasingly convex (peak surface), and as the shape index approaches 1, the surface becomes more concave (pit surface). Thus, subtle curved surface structures can be expressed in numeric form. The curvedness value reflects the degree of curvature and ranges from 0 to 1. As the curvedness value approaches 0, the surface becomes flatter with less curvature. The concepts of the shape index and curvedness value can be easily understood when these 2 parameters are used for the curved surface of the tumor margins (boundary structures between the periphery of the nodule and the surrounding lung). These parameters, the shape index and curvedness value, obtained from the 3D curvature represent the concavoconvex structure of the curved surface and the degree of curvature of the curved surface, which are both determined from the relations between the target pixels and their adjacent pixels. These parameters can be regarded as indices of the uneven distribution of attenuation within the nodule. The histograms of the shape index, curvedness value, and attenuation within the nodule are obtained, and the scale of each histogram serves as a histogram characteristic value.[14] The Fisher linear discriminant classifier is commonly used in pattern classification and is an optimal classifier when the sample distributions are multivariate normal with equal covariance matrices.[15] The linear discriminant classifier was designed by using the histogram features. A leave-one-out procedure was performed to provide a less biased estimation of the performance of the linear discriminant classifier.[16] In this procedure, 1 nodule image is left out from the classifier design group and a linear discriminant function is formulated using the design group. The discriminant score is computed for the case that is left out by using the linear discriminant function obtained. This process cycles through the data set until every

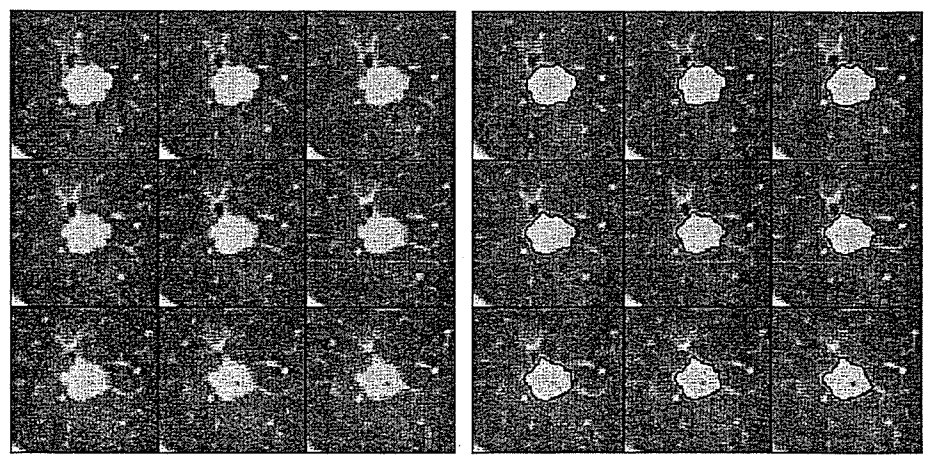

FIGURE 1. Extraction of a pulmonary nodule (case 8).

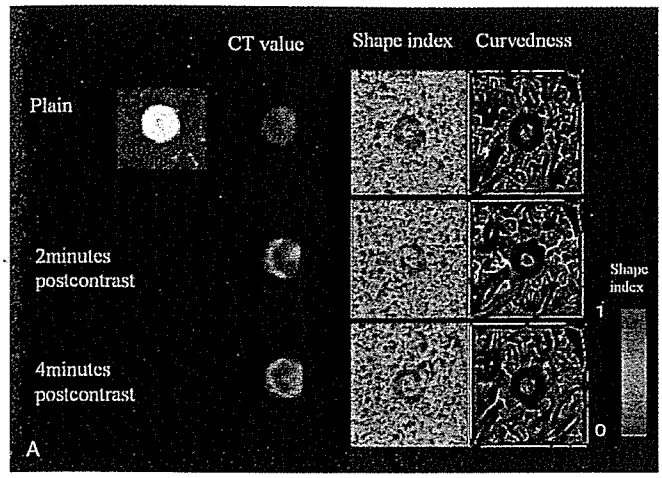

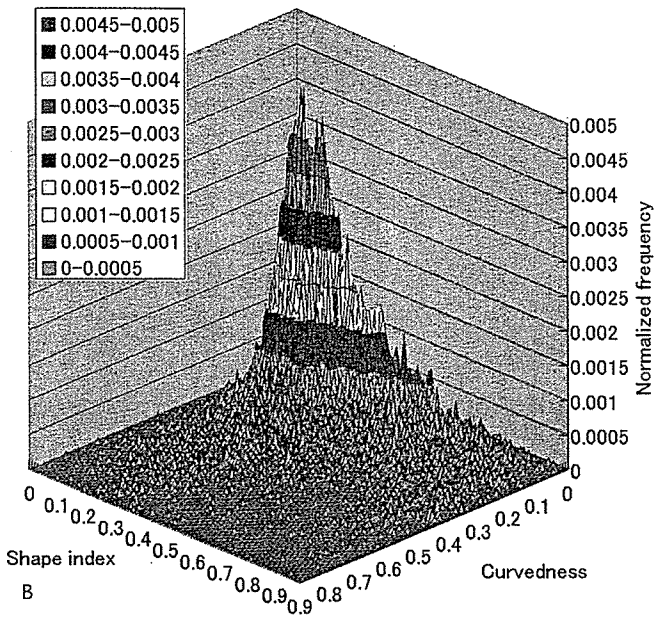

FIGURE 2. A, Characteristic values for a benign nodule (BN; case 37). B, Shape spectra showing a combination of the shape index and curvedness value 4 minutes after contrast enhancement. The *z* axis shows frequency. Most pixels inside a BN have a shape index close to 0 and a low curvedness value. This indicates that pixels inside a BN are mainly of the peak surface type with a smoothly curved surface.

nodule image is used. The overall evaluation time was approximately 4 minutes, including selection of the ROI from the CT images, extraction of the nodule, characterization of the pixels inside the nodule, and calculation of the linear discriminant function scores.

In the present study, each linear discriminant function score was computed from the shape index, curvedness value, and attenuation at each time point: before contrast enhancement and 2 and 4 minutes after the start of enhancement. The malignancy of SPNs was then retrospectively analyzed based on the scores obtained.

In addition, receiver operating characteristic curves were used to evaluate the effectiveness of the linear discriminant score in differentiating between BNs and MNs. Statistical significance was assessed using the unpaired Student *t* test.

Subjects

The subjects in this study were 72 consecutive patients who had undergone chest CT for the detailed examination of SPNs at our department from February 1998 to April 2000. They had only 1 target nodule by CT. Ten patients were not included in the assessment in this study, because CT images of the entire lesion could not be obtained over time (before contrast enhancement and 2 and 4 minutes after contrast enhancement) in these patients because of patient respiratory motion. The remaining 62 patients were evaluated. The mean

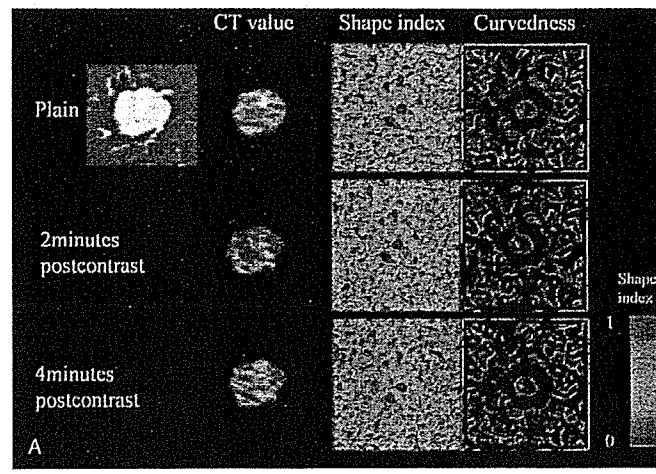

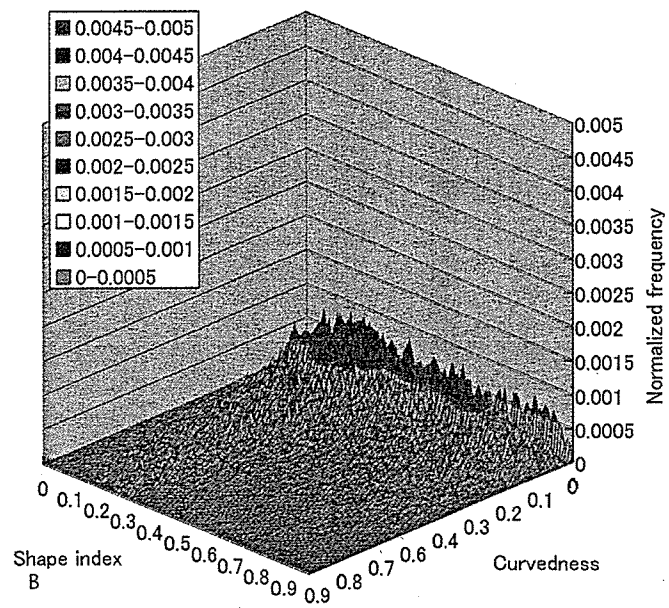

FIGURE 3. A, Characteristic values for a malignant nodule (MN; case 8). B, Shape spectra showing a combination of the shape index and curvedness value 4 minutes after contrast enhancement. Compared with a benign nodule (BN), pixels inside an MN show a wide distribution of shape index values, ranging from 0 to 1, and a high curvedness value. This indicates that pixels inside an MN tend to have pixels other than the peak surface type compared with a BN.

diameter of all nodules was 14 mm (range: 5–25 mm), with a mean diameter of 17 mm (range: 8–25 mm) for MNs and 10 mm (range: 5–17 mm) for BNs. These nodules were classified as 35 malignant lesions (primary lung carcinoma in 33 patients [adenocarcinoma in 31 patients and squamous cell carcinoma in 2 patients] and metastatic pulmonary tumor in 2 patients [breast cancer and colon cancer in 1 patient each]; Table 1) and 27 benign lesions (nonspecific benign lesion in 16 patients, granuloma in 4 patients, hamartoma in 3 patients, organized pneumonia in 1 patient, tuberculoma in 1 patient, pulmonary infarction in 1 patient, and pneumonia in 1 patient; Table 2). The primary lung carcinomas were surgically resected in 29 patients, with the exception of 4 patients with adenocarcinoma. The pathologic stage of the resected tumor was histopathologically graded as stage I in 24 patients, stage II in 1 patient, and stage III in 4 patients. The degree of differentiation of the adenocarcinomas in 27 patients was highly differentiated in 11 patients, moderately differentiated in 14 patients, and poorly differentiated in 2 patients. Metastatic lung tumors were found in these 2 patients based on CT fluoroscopy-guided biopsy. Benign lesions were surgically resected in 4 patients (granuloma, organized pneumonia, tuberculoma, and pulmonary infarction) and identified based on CT fluoroscopy-guided biopsy in 6 patients (hamartoma in 3 patients and granuloma in 3 patients). The nodule disappeared in 1 patient with pneumonia, whereas the remaining 16 patients were diagnosed with a nonspecific benign lesion based on the shape of the lesion and changes in

TABLE 1. Characteristics and Quantitative Characterization of MNS

Patient No.	Age (y)	Sex	Diameter (mm)	Lobe	Linear Discriminant Function			Diagnosis
					Non-Enhanced	2 Min*	4 Min*	
1	5	F	18	RU	1.49	4.42	17.42	W/d AD
2	48	F	18	LU	1.64	10.92	16.95	W/d AD
3	77	M	12	LU	2.4	7.14	24.9	AD
4	68	F	22	RL	4.01	15.77	21.8	M/d AD
5	68	M	11	LU	0.85	6.77	8.18	M/d AD
6	54	F	22	LL	1.96	13.29	14.84	Breast matastasis
7	63	M	12	RU	1.41	9.72	14.77	W/d AD
8	63	M	17	RL	2.25	2.65	9.38	M/d AD
9	55	F	18	LU	3.07	12.34	19.49	M/d AD
10	44	M	15	RU	4.65	4.97	11.71	M/d AD
11	61	F	20	RL	3.21	10.01	17.65	W/d AD
12	84	M	19	LU	3.24	11.07	13.36	AD
13	57	M	15	RU	1.88	9.82	21.61	M/d AD
14	71	M	20	LU	1.11	9.83	13.27	AD
15	61	M	13	RM	1.99	14.51	12.78	Colon matastasis
16	51	F	8	LU	0.93	1.58	9.09	W/d AD
17	51	M	18	LU	3.29	13.02	9.37	P/d AD
18	67	M	15	RU	0.89	12.23	14.58	M/d AD
19	62	F	11	RU	0.87	2.39	22.01	W/d AD
20	61	F	25	RM	1.58	9.56	8.77	W/d AD
21	49	F	19	RM	3.16	13.22	22.45	M/d AD
22	63	F	14	LU	1.32	11.5	9.56	W/d AD
23	45	M	12	RU	1.25	0.58	5.44	M/d AD
24	52	M	18	LU	3.4	9.82	13.59	M/d AD
25	56	F	13	RU	0.28	8.12	17.16	W/d AD
26	53	M	24	RU	2.77	14.89	22.35	M/d AD
27	65	F	23	LU	4.28	16.62	27.11	M/d AD
28	71	F	10	RU	−2.16	5.13	5.27	W/d AD
29	66	F	19	LU	2.68	6.95	18.72	P/d AD
30	40	F	19	RL	2.56	5.87	17.62	M/d AD
31	77	F	16	RU	−0.48	5.56	1.81	M/d AD
32	66	M	15	LL	2.26	23.14	2.95	AD
33	80	M	11	RL	0.13	2.19	22.44	M/d AD
34	68	F	19	RU	5.01	14.78	20.36	W/d AD
35	58	F	24	RL	3.25	15.25	22.56	M/d AD

*Time after administration of contrast agent.

AD indicates adenocarcinoma; F, female; LLL, left lower lobe; LUL, left upper lobe; M, male; M/d, moderately differentiated; P/d, poorly differentiated; RLL, right lower lobe; RML, right middle lobe; RUL, right upper lobe; SQ, squamous cell carcinoma; W/d, well differentiated.